Cross-Modulation of Physicochemical Character of Aglycones in Dinucleoside (3′→5′) Monophosphates by the Nearest Neighbor Interaction in the Stacked State

S. Acharya, P. Acharya, A. Földesi, and J. Chattopadhyaya*

Contribution from the Department of Bioorganic Chemistry, Box 581, Biomedical Center, Uppsala University, S-751 23 Uppsala, Sweden

Received May 8, 2002

Abstract: Each nucleobase in a series of stacked dinucleoside (3′→5′) monophosphates, in both acidic and alkaline pH, shows (^{1}H NMR) not only its own pK_a but also the pK_a of the neighboring nucleobase as a result of cross-modulation of two-coupled π systems of neighboring aglycones. This means that the electronic character of two nearest neighbors are not like the monomeric counterparts anymore; they have simultaneously changed, almost quantitatively, to something that is a hybrid of the two due to two-way transmission of charge (i.e. 3′→5′ as well as 5′→3′). This change is permanent due to total modulation of each others pseudoaromatic character by intramolecular stacking, which can be tuned by the nature of the medium across the whole pH range. The small difference observed in the pK_a of the dimer compared to the monomer is a result of the change in microenvironment in the former. The charge transfer takes place between two stacked nucleobases from the negatively charged end because of the attempt to minimize the charge difference between the two neighboring pseudoaromatic aglycones. Experimental evidence points that the charge transmission in the stacked state takes place by atom−$\pi\sigma$ interaction between nearest neighbor nucleobases in **1**−**6**. The net result of this cross-talk between two neighboring aglycones is a unique set of aglycones in an oligo- or polynucleotide, whose physicochemical property and the pseudoaromatic character are completely dependent both upon the sequence makeup, and whether they are stacked or unstacked. Thus, the physicochemical property of individual nucleobases in an oligonucleotide is determined in a *tunable* manner, depending upon who the nearest neighbors are, which may have considerable implication in the specific ligand binding ability of an aptamer, the pK_a and the hydrogen bonding ability in a microenvironment, in the use of codon triplets in the protein biosynthesis or in the triplet usage by the anticodon−codon interaction.

Introduction

The chemical nature and the exact sequence of the nucleobase in nucleic acids plays a key role in both hydrogen bonding[1] and stacking,[2] leading to replication, transcription, and translation;[2,3] it is also a key element that responds to any environmental changes by protonation, deprotonation, metalation, or binding to any other ligand in intra- and intermolecular interactions.[4−6]

Stacking and hydrogen bonding are two of the most important noncovalent interactions that stabilize and contribute in the self-assembly process of DNA and RNA.[2,7,8,12,13] Although much is known about the hydrogen bonding interactions, very little is understood regarding the nature of stacking interactions.[12,14] Direct experimental evidence,[7,13] leading to the measurement of thermodynamics, supporting the stacking interactions show that the unpaired terminal nucleotides (dangling ends of GC and AU base pairs) increase the stability (by ∼0.5−1.1 kcal
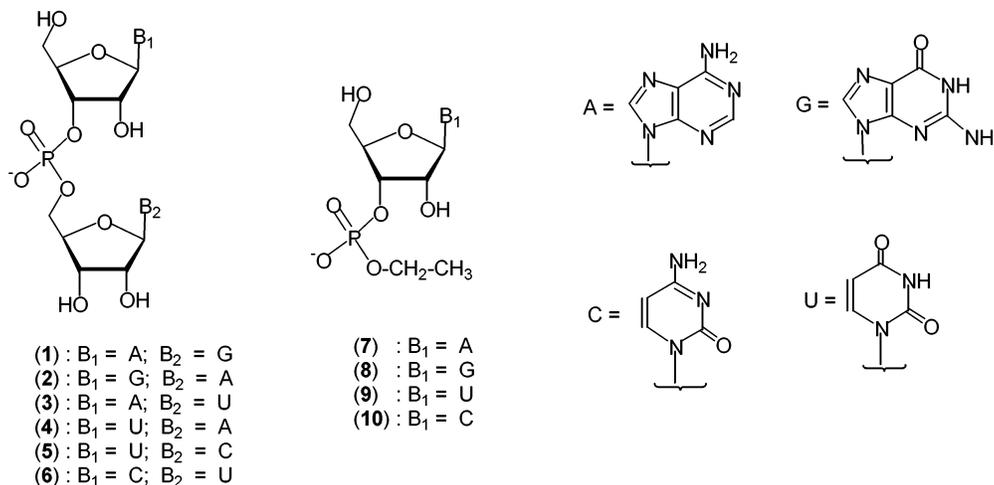
mol^{-1})[7,8] of ribo- and 2′-deoxyoligonucleotide double helix through same strand nearest neighbor stacking interaction.[7,8] It

---

* To whom correspondence should be addressed. Telephone: +4618-4714577. Fax: +4618-554495. E-mail: jyoti@boc.uu.se.

(1) Jeffrey, G. A.; Saenger, W. *Hydrogen Boding in Biological Systems*; Springer-Verlag: Berlin, 1991.

(2) Saenger, W. *Principles of Nucleic Acid Structure*; Springer-Verlag: Berlin, 1988.

(3) Cech, T. R. *Annu. Rev. Biochem.* **1990**, *59*, 543.

(4) (a) Thibaudeau, C.; Plavec, J.; Chattopadhyaya, J. *J. Org. Chem.* **1996**, *61*, 266. (b) The anomeric and the gauche effects are two competing stereoelectronic forces that drive the north (N) (C2′-exo−C3′-endo)⇌south (S) (C2′-endo−C3′-exo) pseudorotational equilibrium in nucleosides. The quantitation of the energetics of pD dependent N ⇌ S pseudorotational equilibria of the pentofuranose moiety in 2′-deoxyribonucleosides (2′-dA, 2′-dG, 2′-dC, T, 2′-dU, 2′-FdU), 1′-imidazolyl-2′-deoxy-β-D-ribofuranose, and ribonucleosides (A, G, C, U, riboT, FU) shows (Thibaudeau, C.; Plavec, J.; Chattopadhyaya, J. *J. Org. Chem.* **1996**, *61*, 266) that the strength of the anomeric effect of the constituent heterocyclic moiety at C1′ is dependent upon the unique *aromatic nature* of the nucleobase, which is tuned by the pD of the medium. The force that drives the protonation⇌deprotonation equilibrium of the heterocyclic nucleobases in nucleosides is transmitted through the anomeric effect to drive the two-state N ⇌ S pseudorotational equilibrium of the constituent furanose: (i) The enhanced strength ($\Delta\Delta H°_{(P−N)}$) of the anomeric effect in the protonated (P) nucleoside compared to the neutral (N) form is experimentally evidenced by the increased preference of sugar for N-type conformation and of the nucleobase in the pseudoaxial orientation in the former by $\Delta\Delta H°_{(P−N)}$ = 3.2 kJ mol^{-1} for dA, 4.9 kJ mol^{-1} for dG, 0.7 kJ mol^{-1} for dU, 2.3 kJ mol^{-1} for dImb, 4.2 kJ mol^{-1} for A, 8.7 kJ mol^{-1} for G, and 2.9 kJ mol^{-1} for C. (ii) In contrast, the S-type sugar conformer, which places the nucleobase in pseudoequatorial orientation, is considerably more preferred in the alkaline medium owing to the weakening of the anomeric effect in the N^1 deprotonated (D) guanine and N^3-deprotonated uracil, 5-fluorouracil, or thymine moieties compared to the neutral counterparts by $\Delta\Delta H°_{(N−D)}$ of 2.1 kJ mol^{-1} for dG, 0.7 kJ mol^{-1} for dU, 0.5 kJ mol^{-1} for T, 0.3 kJ mol^{-1} for FdU, 4.3 kJ mol^{-1} for G, 1.7 kJ mol^{-1} for U, 1.5 kJ mol^{-1} for rT, and 1.5 kJ mol^{-1} for FU. This has allowed us to independently measure the pK_a of constituent heterocyclic nucleobases by the quantitation of the pD-dependent energetics of the two-state N ⇌ S pseudorotational equilibrium.

Chart 1. Dinucleoside (3'→5') Monophosphates Used in This Study: ApG (**1**), GpA (**2**), ApU (**3**), UpA (**4**), UpC (**5**), CpU (**6**), and Their Monomeric Counterparts [ApEt (**7**), GpEt (**8**), UpEt (**9**), and CpEt (**10**)]

(**1**) : B$_1$ = A; B$_2$ = G
(**2**) : B$_1$ = G; B$_2$ = A
(**3**) : B$_1$ = A; B$_2$ = U
(**4**) : B$_1$ = U; B$_2$ = A
(**5**) : B$_1$ = U; B$_2$ = C
(**6**) : B$_1$ = C; B$_2$ = U

(**7**) : B$_1$ = A
(**8**) : B$_1$ = G
(**9**) : B$_1$ = U
(**10**) : B$_1$ = C

has also been shown that the 3'- or 5'-tethered chromophore[9−11] stabilizes DNA−DNA or DNA−RNA duplexes due to inter- or/and intrastrand stacking interactions. One of the distinctive features of stacking interactions has been so far the NMR observed magnetic anisotropy effects, which have allowed us to *qualitatively* estimate the effect of the nearest neighbor.[17−21] Determination of base−base association constants by temperature and/or concentration dependency studies[18,22,23] have also been used in past to understand the stacking interactions. In some nonbiological aromatic systems,[15,16] it has been shown

that, through the introduction of electron-releasing or electron-donating substituents,[15] one can affect the stacking interactions. First unequivocal experimental evidence is presented here by showing that the neighboring aglycones, when stacked, constitute a coupled system, mutually modulating the chemical nature and reactivities.

Our observation on the transmission of the pseudoaromatic character of one base to the next neighbor is based on the comparative studies of dinucleoside (3'→5') monophosphates **1**−**6** (Chart 1) with 3'-ethylphosphates of adenosine, guanosine, uridine, and cytidine **7**−**10**, which are the simplest monomeric models mimicking that of a dimer, in which the stacking is absent. It is systematically demonstrated here that when the partial charge of a neutral nucleobase is specifically altered by either protonation or deprotonation as a result of a change of the pH of the medium (Figures 1−3 and Figures S1−S3 in the Supporting Information), this change, in terms of the $\Delta G°$ corresponding to the pK_a[24,25] ($\Delta G°_{pK_a}$) of the nucleobase (Table 1), is transmitted to the nearest neighbor in the ground state almost quantitatively, thereby modulating the pseudoaromatic character of a stacked neighbor in a sequence-dependent manner. The net result of this charge transfer/electrostatics[12,14,43] is a change of the electronic character of the aglycone, which in turn produces a corresponding shift in $\Delta G°$ of the pseudorotational equilibrium of the constituent sugar conformation in a specific manner (Figure 4A−C), which is consistent with our earlier studies in monomeric nucleosides and nucleotides.[4,5]

Results and Discussion

The dimers **1**−**6** are chosen such that only *one* of the two nucleobases in the molecule can be exclusively protonated or deprotonated at a given pH in order to show the effect of alteration of the electronic character of one aglycon on the other. We have also chosen the isomeric dimer pairs, such as ApU (**3**)/UpA (**4**), ApG (**1**)/GpA (**2**), or UpC (**5**)/CpU (**6**), to show the sequence-specific effect in two possible isomeric aglycone combination, as well as to show the strength of charge transfer/electrostatics[12,14,43] in a sequence-specific manner, i.e. purine−

(5) Acharya, P.; Trifonova, A.; Thibaudeau, C.; Földesi, A.; Chattopadhyaya, J. *Angew. Chem., Int. Ed.* **1999**, *38*, 3645.
(6) For review see: Thibaudeau, C.; Chattopadhyaya, J. *Stereoelectronic Effects in Nucleosides and Nucleotides and Their Structural Implications*; Department of Bioorganic Chemistry, Uppsala University Press (jyoti@boc.uu.se): Uppsala, Sweden, 1999; ISBN 91-506-1351-0, and references therein.
(7) Burkard, M. E.; Kierzek, R.; Turner, D. H. *J. Mol. Biol.* **1999**, *290*, 967, and references therein.
(8) Bommarito, S.; Peyret, N.; SantaLucia, J., Jr. *Nucleic Acid Res.* **2000**, *28*, 1929.
(9) Ossipov, D.; Zamaaratski, E.; Chattopadhyaya, J. *Nucleosides Nucleotides* **1998**, *17 (9−11)*, 1613.
(10) Maltseva, T. V.; Agback, P.; Repkova, M. N.; Venyaminova, A. G.; Ivanova, E. M.; Sandström, A.; Zarytova, V. F.; Chattopadhyaya, J. *Nucleic Acid Res.* **1994**, *22*, 5590.
(11) Ossipov, D.; Pradeepkumar, P. I.; Holmer, M.; Chattopadhyaya, J. *J. Am. Chem. Soc.* **2001**, *123*, 3551.
(12) Hunter, C. A. *J. Mol. Biol.* **1993**, *230*, 1025, and references therein.
(13) The importance of stacking has been identified in DNA polymerase activity and in efficiency of DNA synthesis. For review: Kool, E. T. *Annu. Rev. Biophys. Biomol. Struct.* **2001**, *30*, 1, and references therein.
(14) The interaction of the aromatic rings depends on the stacking geometry: (i) edge-to-face stacked, (ii) offset stacked, and (iii) face-to-face stacked. The offset stacked arrangement minimizes π-electron repulsion and maximizes the interactions in the σ-framework. For review: Hunter, C. A.; Lawson, K. R.; Perkins, J.; Urch, C. J. *J. Chem. Soc., Perkin Trans. 2* **2001**, 651.
(15) Jennings, W. B.; Farrell, B. M.; Malone, J. F. *Acc. Chem. Res.* **2001**, *34*, 885.
(16) The experimental evidence showed that the magnitude of offset stacked interactions can be dictated by the geometry of the stacked components, which, in turn, is influenced by the nature of ring substituents. Rashkin, M. J.; Waters, M. L. *J. Am. Chem. Soc.* **2002**, *124*, 1860, and refs 1, 2, and 8 therein.
(17) Altona, C. in *Structure and Conformation of Nucleic Acids and Protein-Nucleic Acid Interactios*; Sundaralingam, M., Rao, S. T., Eds.; University Park Press: Baltimore, MD, 1975; p 613.
(18) Lee, C.-H.; Ezra, F. S.; Kondo, N. S.; Sarma, R. H.; Danyluk, S. *Biochemistry* **1976**, *15*, 3627.
(19) Topal, M. D.; Warshaw, M. M. *Biopolymers* **1976**, *15*, 1775.
(20) Kolondny, N. H.; Neville, A. C.; Coleman, D. L.; Zamecnik, P. C. *Biopolymers* **1977**, *16*, 259.
(21) Cox, R. A. *Biochem. J.* **1966**, *100*, 148.
(22) Schmidt, A.; Kindermann, M. K.; Vainotalo, P.; Nieger, M. *J. Org. Chem.* **2000**, *64*, 9499.
(23) Chan, S. I.; Nelson, J. H. *J. Am. Chem. Soc.* **1969**, *91*, 168.
(24) Perrin, D. D.; Dempsey, B.; Serjeant, E. P. *pK$_a$ Prediction for Organic Acids and Bases*; Chapman and Hall: New York, 1981.
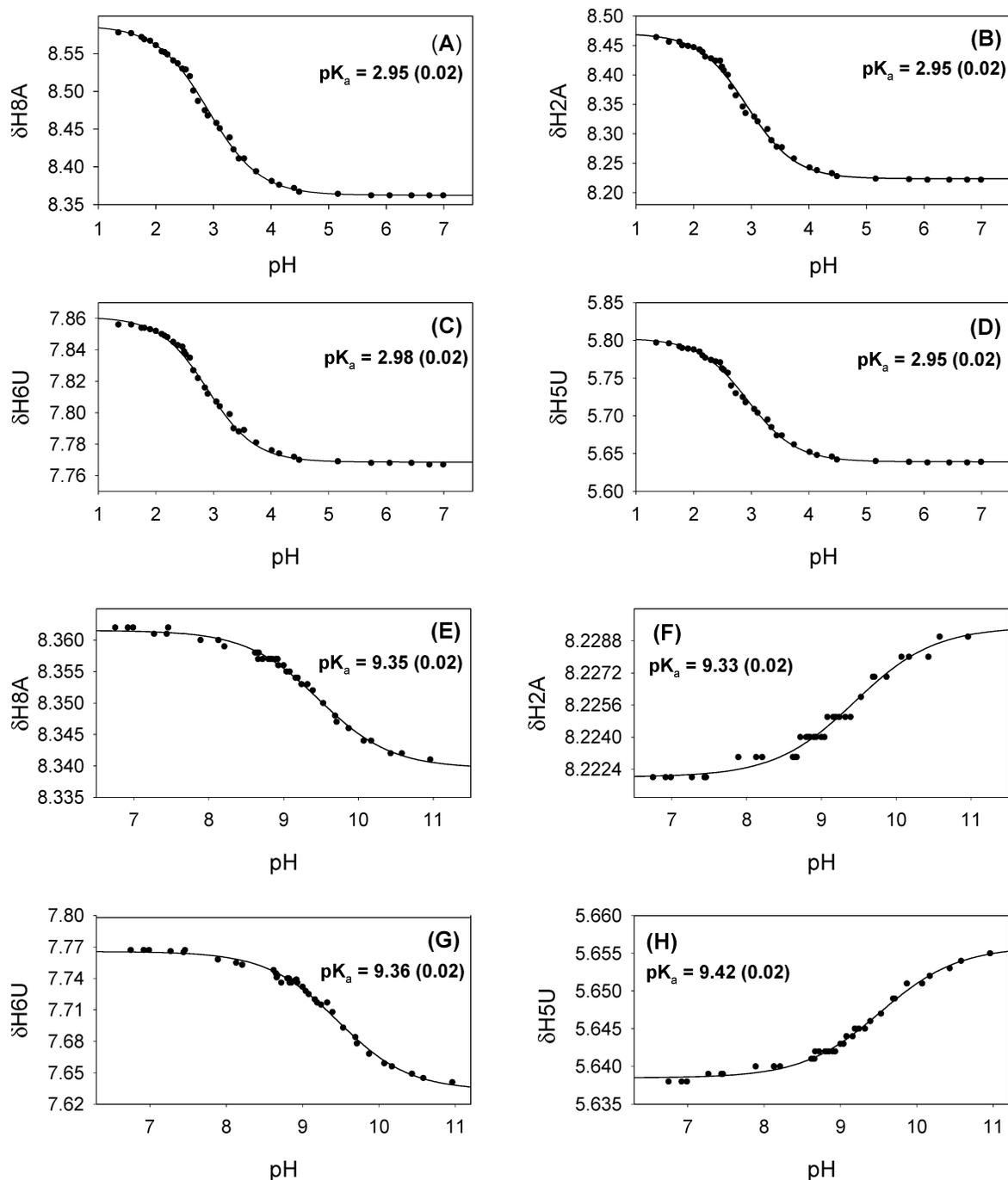(25) Sharp, K. A.; Honig, B. *Annu. Rev. Biophys. Chem.* **1990**, *19*, 301.

Figure 1. (A−D) pH-dependent ^{1}H chemical shift of aromatic protons (H8A, H2A, H6U, H5U) of ApU within the pH values of $1.35 \leq$ pH ≤ 6.99. Chemical shift variations at 36 different pH values ($1.35 \leq$ pH ≤ 6.99) have been measured in an interval of 0.1−0.2 pH units to obtain the sigmoidal curves. pK_a values obtained from Hill plot (see the Experimental Section for details) of H8A, H2A, H6U and H5U are shown in respective graphs. (E−H) pH-dependent ^{1}H chemical shift of aromatic protons (H8A, H2A, H6U, H5U) of ApU within the pH values of $6.99 \leq$ pH ≤ 10.96. Chemical shift variations at 39 different pH values ($6.99 \leq$ pH ≤ 10.96) have been measured in an interval of 0.1−0.2 pH units to obtain the sigmoidal curves in all cases. pK_a values (with corresponding error in the parenthesis) obtained from Hill plot of H8A, H2A, H6U and H5U are shown in the respective graphs. Similar graphs for rest of the compounds are shown in Figure S1 in the Supporting Information.

pyrimidine (**3** and **4**), purine−purine (**1** and **2**), and pyrimidine−pyrimidine (**5** and **6**). The plots of pH-dependent chemical shift of aromatic protons of the aglycones of dimers **1**−**6** demonstrate typical titration curves, showing how the effect of protonation or deprotonation of a specific nucleobase is transmitted to alter the electronic property of the neighboring aglycone: Table 1 summarizes the results of pH-dependent titration giving pK_a and the corresponding $\Delta G^\circ_{pK_a}$ for **1**−**10** [Figure 1 for titration

curves, Figure 2 for corresponding Hill plots, and Figure 3 for the fraction of protonation/deprotonation at different pH for ApU (**3**) as a model example, and see Figures S1−S3 in the Supporting Information for similar graphs corresponding to rest of the compounds **1**−**10**].

Thus, the pH-dependent titration of ApU (**3**) in the acidic range (pH 1.5−7.0) gave the pK_a (Figure 2A−D) of N^1 of adenine-9-yl (A) not only by the sigmoidal shift (Figure 1A−
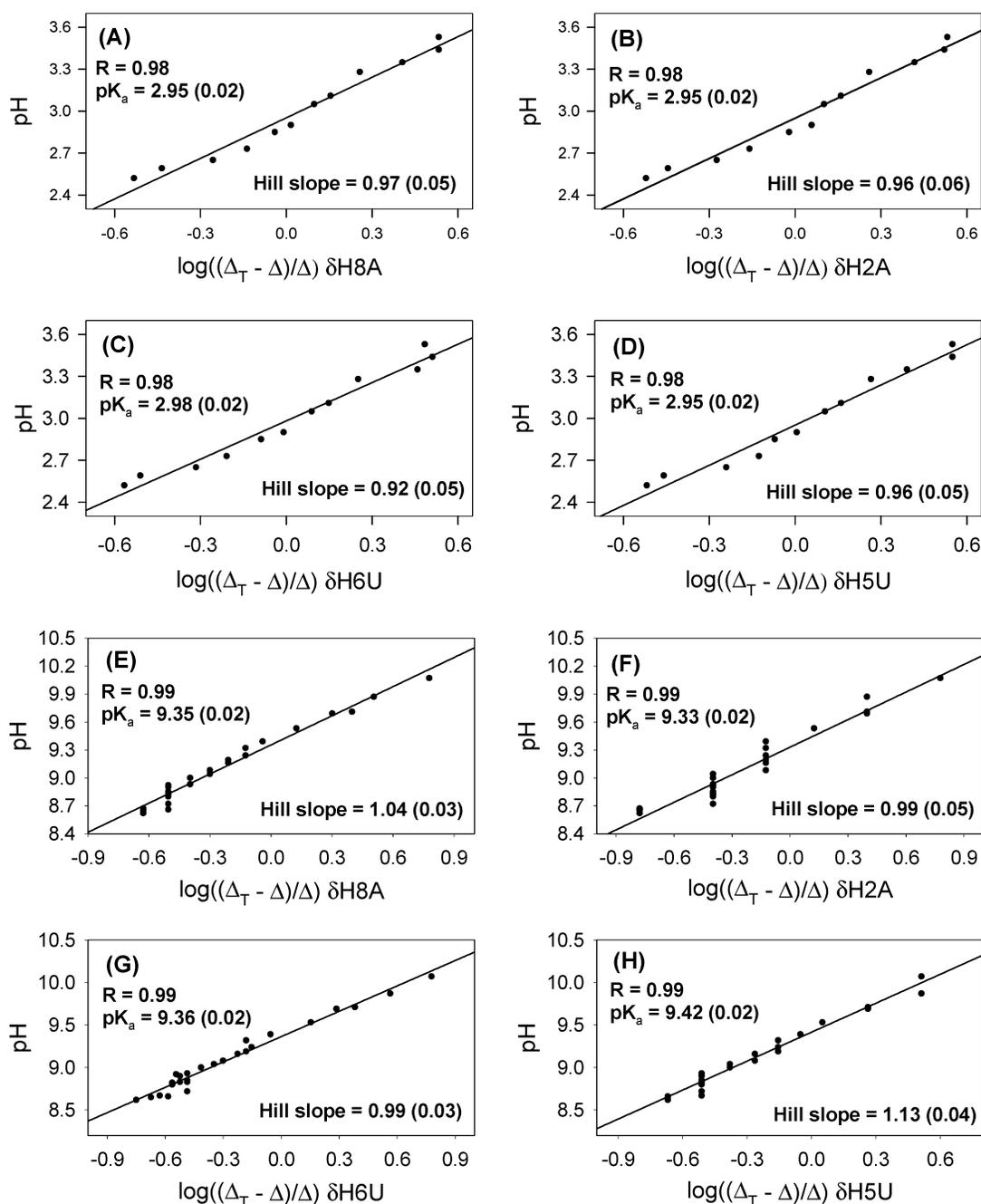
Figure 2. Hill plot analyses performed by plotting pH as a function of $\log((\Delta_T - \Delta_{P/D})/\Delta_{P/D})$ to calculate pK_a and Hill slope (see the Experimental Section for details). The total change in chemical shift between neutral and protonated or deprotonated state is denoted as Δ_T (ppm). Panels A−D show the Hill plots for δH8A, δH2A, δH6U, δH5U of ApU in the $1.35 \leq pH \leq 6.99$. Δ_T for H8A ($1.35 \leq pH \leq 6.99$) = 0.216 ppm. Δ_T for H2A ($1.35 \leq pH \leq 6.99$) = 0.242 ppm. Δ_T for H6U ($1.35 \leq pH \leq 6.99$) = 0.089 ppm. Δ_T for H5U ($1.35 \leq pH \leq 6.99$) = 0.159 ppm. The values of correlation coefficient R, pK_a obtained from each Hill plot analysis, and the Hill slope of δH8A, δH2A, δH6U, and δH5U are shown in the respective graphs. The error of pK_a and Hill slope are given in the parentheses. Panels E−H show the Hill plots for δH8A, δH2A, δH6U, δH5U of ApU in the $6.99 \leq pH \leq 10.96$. Δ_T for H8A ($6.99 \leq pH \leq 10.96$) = 0.021 ppm. Δ_T for H2A ($6.99 \leq pH \leq 10.96$) = 0.007 ppm. Δ_T for H6U ($6.99 \leq pH \leq 10.96$) = 0.126 ppm. Δ_T for H5U ($6.99 \leq pH \leq 10.96$) = 0.017 ppm. The values of correlation coefficient R, pK_a obtained from each Hill plot analysis, and the Hill slope values of δH8A, δH2A, δH6U, and δH5U are shown in the respective graphs. The error of pK_a and Hill slope are given in the parentheses. Similar graphs for rest of the compounds are shown in Figure S2 in the Supporting Information.

D) of its own δH2A (pK_a 2.95) and δH8A (pK_a 2.95), but also by the shift of δH5U (pK_a 2.95) and δH6U (pK_a 2.98) of the neighboring uracil-1-yl (U) moiety. Similarly, in the alkaline range (pH 7.0−11.5), quite expectedly, the titration curves (Figure 1E−H) of δH5U (pK_a 9.42) and δH6U (pK_a 9.36) of uracil-1-yl (U) showed the pK_a (Figure 2E−H) of N^3−H deprotonation. Remarkably, this was also exhibited by the

sigmoidal shift of δH2A (pK_a 9.33) and δH8A (pK_a 9.35) of the neighboring adenine-9-yl aglycon. Thus, adenine-9-yl moiety uniquely shows the pK_a of N^3 of uracil-1-yl in the alkaline pH, and uracil-1-yl shows the pK_a of N^1 of adenine-9-yl in the acidic pH in ApU (**3**) as a result of charge transmission from one nucleobase to the other due to their stacked geometry. This two-way, i.e. 3′→5′ as well as 5′→3′, cross-modulation of the
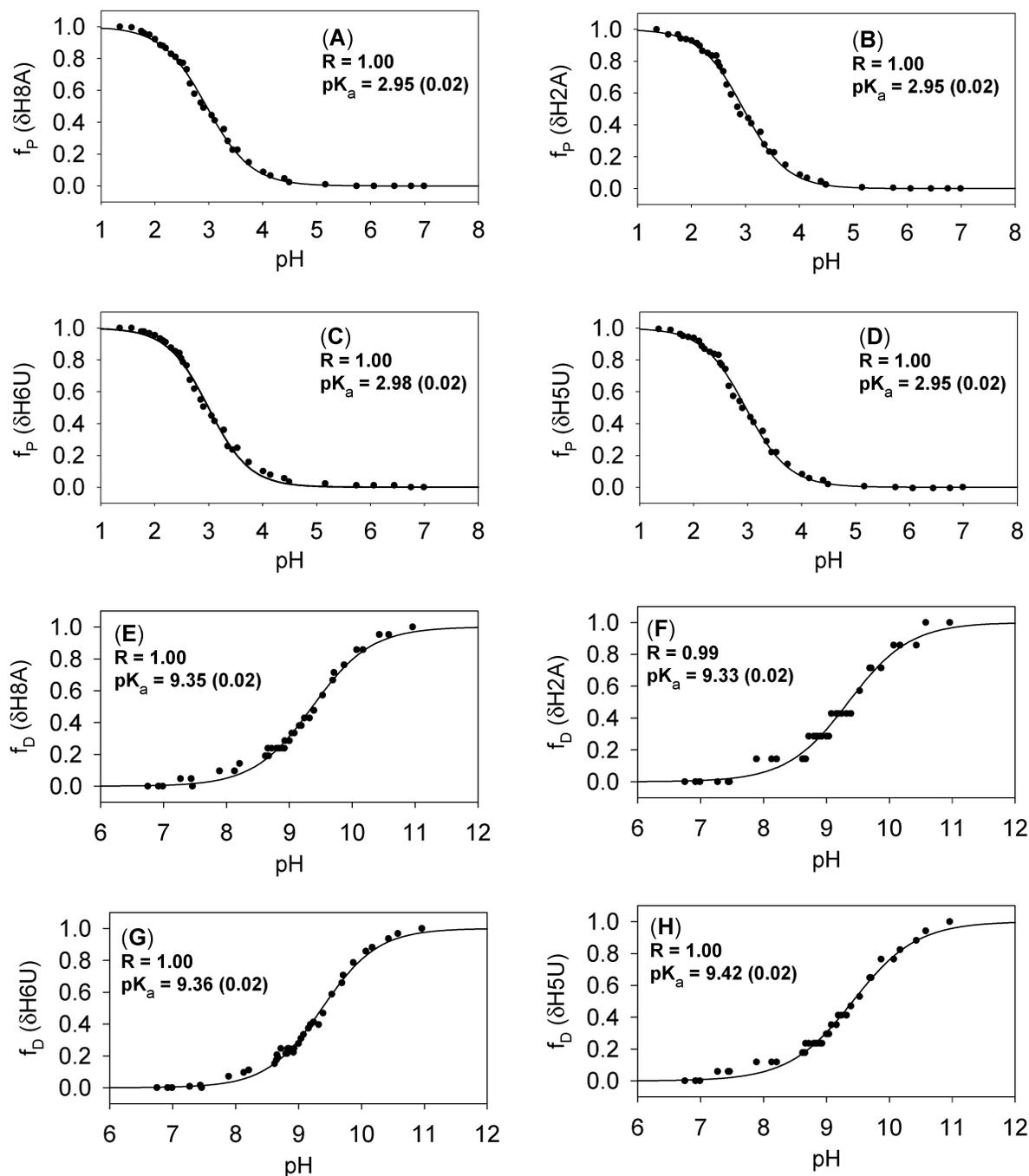
Figure 3. (A–D) pH-dependent fraction protonation (f_P; see Experimental Section for details) of aromatic protons (H8A, H2A, H6U, H5U) of ApU within the pH values of $1.35 \leq pH \leq 6.99$. Δ_T (in ppm) is the total change in chemical shift between neutral and protonated/deprotonated states. $\delta_{neutral}$ (in ppm) is the chemical shift at neutral state. $\delta_{neutral}$ (8.362) of H8A is subtracted from δ_{obs} at each pH value of H8A and divided by Δ_T (0.216) to get the value of f_P. $\delta_{neutral}$ (8.222) of H2A is subtracted from δ_{obs} at each pH values of H2A and divided by Δ_T (0.242) to get the value of f_P. $\delta_{neutral}$ (7.767) of H6U is subtracted from δ_{obs} at each pH values of H6U and divided by Δ_T (0.089) to get the value of f_P. $\delta_{neutral}$ (5.639) of H5U is subtracted from δ_{obs} at each pH values of H5U and divided by Δ_T (0.159) to get the value of f_P. The values of correlation coefficient R and pK_a (with corresponding error in the parentheses) obtained from Hill plot of H8A, H2A, H6U, and H5U are shown in the respective graphs. Panels E–H show pH-dependent fraction deprotonation (f_D; see Experimental Section for details) of aromatic protons (H8A, H2A, H6U, H5U) of ApU within the pH values of $6.99 \leq pH \leq 10.96$. $\delta_{neutral}$ (8.362) of H8A is subtracted from δ_{obs} at each pH values of H8A and divided by Δ_T (0.021) to get the value of f_D. $\delta_{neutral}$ (8.222) of H2A is subtracted from δ_{obs} at each pH values of H2A and divided by Δ_T (0.007) to get the value of f_D. $\delta_{neutral}$ (7.767) of H6U is subtracted from δ_{obs} at each pH values of H6U and divided by Δ_T (0.126 ppm) to get the value of f_D. $\delta_{neutral}$ (5.638) of H5U is subtracted from δ_{obs} at each pH values of H5U and divided by Δ_T (0.017) to get the value of f_D. The values of correlation coefficient R and pK_a (with corresponding error in the parentheses) obtained from Hill plot of H8A, H2A, H6U, and H5U are shown in the respective graphs. Similar graphs for rest of the compounds are shown in Figure S1 in the Supporting Information.

pseudoaromatic character of the nucleobase from one to the other was also observed for UpC (**5**) and CpU (**6**) at pH range from 1.0 to 11.7.

For ApG (**1**) and GpA (**2**), we could clearly observe the transmission of pseudoaromatic character of conjugate base of guanine-9-yl to adenine-9-yl in the alkaline pH (Table 1). Due to close pK_a of guanine-9-yl (pK_a 1.58 for N^7) and adenine-9-yl ($pK_a \sim 3$ for N^1), the titration curves in the acidic pH were overlapping, which did not allow us to delineate their respective pK_as and therefore the cross-modulation of the pseudo-

Table 1. pK_a of Nucleobase from Hill Plot[a] Analyses and Corresponding Free Energy of Protonation/Deprotonation[24,25] at pK_a (ΔG°_{pKa}, in kJ mol^{-1})[b] for Compounds **1**−**10**

compd		δH8G		δH8A		δH2A		δH6C		δH6U		δH5C		δH5U	
		pK_a	ΔG°_{pKa}	pK_a	ΔG°_{pKa}	pK_a	ΔG°_{pKa}	pK_a	ΔG°_{pKa}	pK_a	ΔG°_{pKa}	pK_a	ΔG°_{pKa}	pK_a	ΔG°_{pKa}
ApG (**1**)	5′ A^{H+}	1.64	9.0	2.88	16.4	2.83	16.2	-	-	-	-	-	-	-	-
	3′G$^-$	9.42	53.7	9.71	55.4	9.65	55.1	-	-	-	-	-	-	-	-
GpA (**2**)	5′G$^-$	9.17	52.4	9.11	52.0	9.11	52.0	-	-	-	-	-	-	-	-
	3′A^{H+}	1.68	9.6	3.22	18.4	2.94	16.8	-	-	-	-	-	-	-	-
ApU (**3**)	5′A^{H+}	-	-	2.95	16.8	2.95	16.8	-	-	2.98	17.0	-	-	2.95	16.8
	3′U$^-$	-	-	9.35	53.3	9.33	53.2	-	-	9.36	53.4	-	-	9.42	53.7
UpA (**4**)	5′U$^-$	-	-	_c	_c	_c	_c	-	-	9.09	51.9	-	-	9.09	51.9
	3′A^{H+}	-	-	3.07	17.5	3.06	17.5	-	-	3.12	17.8	-	-	3.01	17.2
UpC (**5**)	5′U$^-$	-	-	-	-	-	-	9.14	52.1	9.06	51.7	9.06	51.7	9.04	51.6
	3′C^{H+}	-	-	-	-	-	-	3.71	21.2	3.71	21.2	3.71	21.2	3.71	21.2
CpU (**6**)	3′C^{H+}	-	-	-	-	-	-	3.56	20.3	3.48	19.9	3.58	20.4	3.58	20.4
	5′U$^-$	-	-	-	-	-	-	9.18	52.4	9.21	52.5	9.18	52.4	9.25	52.8
ApEt (**7**)	A^{H+}	-	-	3.11	17.7	3.10	17.7	-	-	-	-	-	-	-	-
GpEt (**8**)	G$^-$	9.25	52.8	-	-	-	-	-	-	-	-	-	-	-	-
UpEt (**9**)	U$^-$	-	-	-	-	-	-	-	-	9.44	53.9	-	-	9.43	53.8
CpEt (**10**)	C^{H+}	-	-	-	-	-	-	3.84	21.8	-	-	3.84	21.8	-	-

[a] All pK_a values have been calculated from hill plot[4,30] (see experimental part for details) and the average error of the analyses between ±0.01 and ±0.04. [b] all values for ΔG°_{pKa} (given in columns 4, 6, 8, 10, 12, 14, and 16) have been calculated using equation, $\Delta G^\circ_{pKa} = 2.303RT^*pK_a$, and the error of analyses is between ±0.1 and ±0.2 kJ mol^{-1}. [c] δH8A and δH2A of the adenine-9-yl in UpA (**4**) did not show any titration profile (legends of Figures S1−S3 in the Supporting Information) as a function of pH in alkaline range.

aromatic character of guanine-9-yl and adenine-9-yl separately.

The pH titration of UpA (**4**) in the acidic range (pH 1.5−7.0) show the pK_a of N^1 of adenine-9-yl from its own δH2A (pK_a 3.06) and δH8A (pK_a 3.07) as well as from δH5U (pK_a 3.01) and δH6U (pK_a 3.12) of the neighboring uracil-1-yl. However, in the alkaline range (pH 7.0−11.5), pK_a of N^3 of uracil-1-yl in **4** is shown by both δH5 (pK_a 9.09) and δH6 (pK_a 9.09) of uracil-1-yl, nevertheless, δH2 and δH8 of neighboring adenine-9-yl remains nonresponding (see legends of Figure S1j in the Supporting Information), so it has been concluded that no effective charge transfer/electrostatics[12,14,43] was taking place because the two nucleobases are almost *destacked* in the alkaline pH (Figure 4D and Table 1).

The change of sugar conformation in the dimers **1**−**6** as a result of differential electrostatics owing to the transmission of charge[26,27] between two neighboring aglycones has been accurately estimated (as well as those of the monomeric counterparts **7**−**10**, for comparison) through a detailed analysis of all pH-dependent endocyclic $^3J_{HH}$ coupling constants (Figure 4A−C and Table S1 in the Supporting Information), which has led us to calculate the pH-dependent free energy of stacking (-0.3 kJ mol^{-1} $\leq \Delta G^\circ_{stacking} \leq -3.6$ kJ mol^{-1}), in comparison with the monomeric counterparts, at different pH (Figure 4D and Experimental Section). The estimated free energy of stacking for six dimers **1**−**6** through our $^3J_{HH}$ analysis (Figure 4D) at neutral pH is completely consistent[28] with those obtained by thermodynamic analysis (based on T_m analysis) of short RNA helix with dangling bases,[7] thereby showing the validity of our above approach for determination of the strength of stacking across the whole pH range. Comparison of the sugar conformational changes (Np) in the dimer with that of the monomer

(NpEt) *at different pH* shows (Figure 4A−C) that the alteration of the pseudoaromatic character of the nucleobase due to nearest neighbor stacking interaction in the dimer has indeed changed the constituent pentose-sugar conformation, as would be expected from the earlier studies,[4−6] which have shown that the N $\rightleftarrows$ S pseudorotational equilibrium of the sugar is indeed steered by the *pH-dependent modulation of the pseudoaromatic character of the constituent aglycone* as a result of tunable stereoelectronic $n_{O4'} \rightarrow \sigma^*_{(C1'−N9/1)}$ charge transfer.[4−6] Since the sugar conformation change in the dimers **1**−**6** is found to be

(27) Among ApG$^-$ and G$^-$pA, 3′G$^-$ in the former is relatively a better donor (compare $\Delta\delta$ with those of the corresponding deprotonated monomeric units). However, 3′A in G$^-$pA can more efficiently back-donate[44] the charge to 5′G$^-$, as evident from larger downfield shift of $\Delta\delta$ (H8A) compared to that ApG$^-$ (Figures S4A1 and S4A2 in the Supporting Information). So the efficiency of back-donation from A, depends on the forward donation of charge from G$^-$. Hence, the charge-transfer process of ApG$^-$ is more efficient than G$^-$pA, which is also consistent with the fact that the former is relatively more stacked among the two (compare the $\Delta\Delta G^\circ$ in Figure 4D). Almost no change in the chemical shifts of H8A and H2A is found in A^{H+}pU compared to those of A^{H+}pEt (Figures S4B1 and S4C1 in the Supporting Information). However, relative upfield shift of H8A and H2A in UpA^{H+} compared to those in A^{H+} shows 5′U (in UpA^{H+}) is better donor than 3′U (in A^{H+}pU). The change of the chemical shift of H6U in ApU$^-$ is similar to that in U$^-$pA. (Figures S4B2 and S4C2 in the Supporting Information). Nevertheless, 3′A in U$^-$pA can back-donate the charge to U more favourably than for 5′A in ApU$^-$, which is evident from the fact that Ap in ApU$^-$ is more negatively charged (i.e. shielded) than in U$^-$pA. So the average charge transfer/electrostatics[12,14,43] in ApU$^-$ is most efficient because it is relatively more stacked than U$^-$pA (compare the $\Delta\Delta G^\circ$ in Figure 4D). As 3′C^{H+} is better acceptor, it can attract charge from 5′U in UpC^{H+}. However, average donor−acceptor property in UpC^{H+} is less as 5′U is a poor donor. Similarly the charge donation efficiency of 3′U (in C^{H+}pU) is better than in 5′U (in UpC^{H+}), nevertheless, acceptance property of 5′C^{H+} is poor. So on average the efficiency of donor−acceptor properties in both UpC^{H+} and C^{H+}pU are poor (Figures S4D1 and S4E1 in the Supporting Information). On the other hand, 5′U$^-$ in U$^-$pC is a better donor, but the 3′C is a poor acceptor (Figures S4D2 and S4E2 in the Supporting Information). However, 3′U$^-$ is relatively an efficient donor, and the acceptor capacity of 5′C is relatively better, which makes the most proficient charge transfer/electrostatics[12,14,43] in CpU$^-$ compared to UpC^{H+}, C^{H+}pU, and U$^-$pC, which is also consistent with the fact that CpU$^-$ is the most staked among all pyrimidine−pyrimidine dimers (compare the $\Delta\Delta G^\circ$ in Figure 4D).

(26) It has been assumed that the observed stabilization due to stacking by the same strand in the nearest neighbor model in DNA and RNA duplexes is a result of charge transfer/electrostatics[12,14,43] between donor and acceptor. It has also been suggested that the partial charges of two nearest neighbor nucleobase plays important role in their donor−acceptor properties.[12,43] Such resonance-assisted stabilization will have impact in the donor−acceptor properties resulting in H-bonding abilities[41] and pK_a perturbation.[30−36]

(28) The strength of stacking interaction[7] in terms of the duplex stabilization ($-\Delta G^\circ_{stacking}$) by either the 3′- or the 5′-dangling end in short RNA helix is as follows:[7] (i) strong interaction, ≥ 3.3 kJ mol^{-1}; (ii) intermediate, ≤ 2.9 kJ mol^{-1}, to weak interaction, ≤ 1.7 kJ mol^{-1}; (iii) poorly stacked (or almost unstacked) interaction, ≤ 1.3 kJ mol^{-1}. *Moreover, these values are well-correlated with free energy stabilization of stacking at helix termini in larger RNA and are consistent with our present studies (Figure 4D) too.*
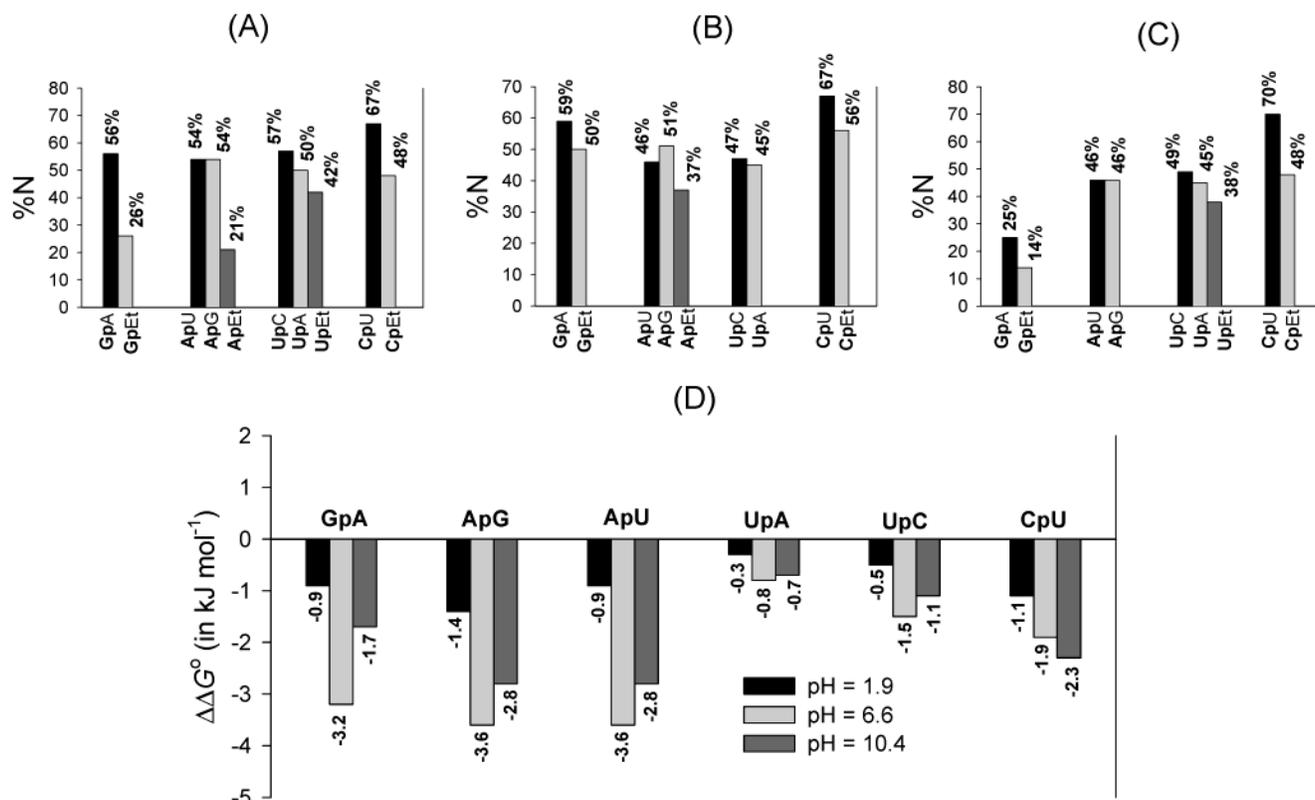
Figure 4. (A−C) Bar plot of the percentage population of the N-type conformation [%N, calculated using all endocyclic $^3J_{HH}$ with the help of PSEUROT (v5.4)[6]] of 3'-nucleotidyl moiety (in bold) in 3'−5' dinucleoside monophosphate (**GpA**, **ApG**, **ApU**, **UpA**, **UpC**, and **CpU**; see Chart 1) as well as for the corresponding monomeric nucleoside 3'-ethyl phosphate (**GpEt**, **ApEt**, **UpEt**, and **CpEt**; see Chart 1) at neutral (pH = 6.6), acidic (pH = 1.9) and alkaline (pH = 10.4) state, respectively. Approximate relation %N = 100(7.9 − $^3J_{1'2'}$)/6.9 is used for **ApG** in acidic region (pH = 1.9), because PSEUROT (v5.4) could not be performed due to unavailability of both $^3J_{2'3'}$ and $^3J_{3'4'}$ (see Experimental Section and Table S1 in the Supporting Information for details). Panel D shows the free energy of stacking ($\Delta\Delta G° \cong \Delta G°_{stacking}$, in kJ mol^{-1}) for **1**−**6** at neutral (pH = 6.6), acidic (pH = 1.9), and alkaline (pH = 10.4) state. $\Delta G°_{stacking}$ has been estimated using relation: $\Delta\Delta G° \cong \Delta G°_{stacking} = [\Delta G°_{N/S(298K)}]_{NpN'} - [\Delta G°_{N/S(298K)}]_{NpEt}$, where **NpN'** and **NpEt** signify 3'-nucleotidyl moiety (in bold) of 3'−5' dinucleoside monophosphate (**GpA**, **ApG**, **ÅpU**, **UpA**, **UpC**, and **CpU**; see Chart 1) and nucleoside 3'-ethyl phosphate (**NpEt** with N = A, G, U, and C; see Chart 1), respectively. The corresponding free energy of the N ⇌ S pseudorotational equilibrium,[6] $\Delta G°_{N/S(298K)}$ (in kJ mol^{-1}), has been calculated for **1**−**6** at acidic (pH = 1.9), neutral (pH = 6.6), and alkaline (pH = 10.4) state, using Gibb's equation: $\Delta G°_{N/S(298K)} = -RT \ln K$, where $K = (x_N/x_S)$; x_N and x_S are the mole fraction of N-type and S-type pseudorotamer, respectively. Hence, the negative $\Delta G°_{N/S(298K)}$ implies relatively more N-type conformational population, so more stabilization due to stacking[17,18] (see the Experimental Section and Table S1 in Supporting Information for details).

strictly *sequence-dependent*, this suggests that the observed modulation of the pseudoaromatic property of a specific aglycone in the dimer, in comparison with that of the monomer, is a result of the stacking interaction with the next neighbor across the whole pH range from 1.5 to 11.5 (Figure 4A−D). Hence, the shift of the stacking⇌destacking equilibrium constitutes an ON−OFF switch for the transmission of the pseudoaromatic character to the nearest neighbor. This is further evidenced by $\Delta G°_{pK_a}$ (Table 1) of the constituent nucleobases of the dimers, which are different from that of the corresponding monomeric unit because of differential microenvironment (compare $\Delta G°_{pK_a}$ of A^{H+}pU, 16.8 ± 0.1 kJ mol^{-1} with that of A^{H+}pEt, 17.7 ± 0.2 kJ mol^{-1}; $\Delta G°_{pK_a}$ of U$^-$pC, 51.7 ± 0.1 kJ mol^{-1} with that of U$^-$pEt, 53.9 ± 0.2 kJ mol^{-1}; $\Delta G°_{pK_a}$ of C^{H+}-pU, 20.3 ± 0.2 kJ mol^{-1} with that of C^{H+}pEt, 21.9 ± 0.2 kJ mol^{-1}).

Conclusions

The dimerization shift study[17−19] (Figure S5 in the Supporting Information), as well as the sugar conformation analysis using all endocyclic $^3J_{HH}$ showed (Figure 4D) that the above dimers are most stacked in the neutral form [except for CpU (**6**), where CpU$^-$ is relatively more stacked than its neutral form]. Our new

finding is that their stacking propensity does *not* become nil in the ionic forms at room temperature (Figure 4D); it only partly decreases, and even then there are examples when the stacking remains unaltered. In general, the extent of 3'→5' stacking decreases in the following order:[2,7] Purine−purine ≅ purine−pyrimidine > pyrimidine−pyrimidine > pyrimidine−purine. It has emerged that it is the stacking interactions between adjacent bases (sequence-stacking rule)[2] which gives rise to the stable, single-stranded helical structure: Thus, poly(A) is mainly helical, whereas poly(U) is predominantly random coil at room temperature. Since we can successfully measure the pK_a of both nucleobases from either of the aglycones in the dimers **1**−**6**, it shows that the aglycones in the dimeric forms constitute a *coupled system* right across the whole pH range, 1.5−11.5 due to two-way transmission of charge (i.e. 3'→5' as well as 5'→3').[27] The magnitude of the chemical shift change in any of the aromatic protons in either of the two coupled aglycones differs in a *variable* manner[27] depending upon the geometry of stacking,[12] partial charge of the heteroatom, and the sequence, which is evident from the relative chemical shift change ($\Delta\delta$) upon protonation or deprotonation [$\Delta\delta = \delta_N - \delta_{P/D}$, in parts per million; N, P, D stands for neutral, protonated, and deprotonated states in Figure S4 in the Supporting Information].

Thus, this variable $\Delta\delta$, observed for various aromatic protons, offers direct proof that the partial stacking (in the ionic states as well as in the pyrimidine−pyrimidine dimers) gives a *nonuniform* charge transfer[27]/electrostatics[12,14,43] to various atoms in a stacked aglycone (Figure S4 and Table S1 in the Supporting Information) because of offset stacking[16] involving atom−$\pi\sigma$ interaction.[12] The net result of such physicochemical cross-modulation of the pseudoaromatic character of each other in any two neighboring aglycones is that they may influence each other's property in a microenvironment (such as specific ligand binding ability of an aptamer,[29] pK_a,[30−35] hydrogen bonding ability,[36] use of a degenerate codon triplets in the protein biosynthesis,[37] triplet usage by the anticodon−codon interaction[38]) in a *tunable* manner, depending both upon the sequence, medium, and whether they are stacked or unstacked in various folded states. Thus, this cross-talk produces a unique set of aglycones with novel physicochemical property in an oligo- or polynucleotide, which is completely different from the corresponding monomers due to the nearest neighbor effect. It is likely that this stacking-sequence based cross-modulation of the pseudoaromatic character by charge transfer[27]/electrostatics[12,14,43] to the nearest neighbor will be more pronounced in helical double strands than in the single strands because of the restricted flexibility of the former, which is consistent with what is observed in the long-distance charge transport.[39,40]

Experimental Section

(A) pH-Dependent ^{1}H NMR Measurement. All NMR experiments were performed in a Bruker DRX-500 spectrometer operating at 500.1326 MHz for proton observation. The NMR sample for compounds **1**−**10** (Chart 1) were prepared in D_2O solution (concentration of 1 mM in order to rule out any chemical shift change owing to self-association[20]) with $\delta_{DSS} = 0.015$ ppm as internal standard. All pH-dependent NMR measurements have been performed at 298 K. The pH values [pH = pD − 0.4 for the correction of deuterium effect] corresponds to the reading on a pH meter equipped with a calomel microelectrode (in order to measure the pH inside the NMR tube) calibrated with standard buffer solutions (in H_2O) of pH 4, 7, and 10. The pD of the sample has been adjusted by simple addition of microliter volumes of D_2SO_4 and NaOD solutions (0.5, 0.1, and 0.01 M). The assignments for all compounds have been performed on the basis of selective homo- (^{1}H) and heteronuclear (^{31}P) decoupling experiments. All spectra have been recorded using 64 K data points and 64 scans for ^{1}H and 128 K data points and 128 scans for ^{31}P.

pH-dependent $^3J_{HH}$ (±0.1 Hz) has been precisely estimated (Table S1 in the Supporting Information) by the simulation of the experimental spectra using using the DAISY program package (supplied by Bruker spectrospin). See section E for further details of PSEUROT (v5.4)[6] calculations using simulated endocyclic $^3J_{HH}$.

(B) pK_a Determination. The pH-dependent [over the range of pH 0.3−7.0 (acidic range) and 7.0−11.6 (alkaline range), with an interval of pH 0.1−0.2] ^{1}H chemical shift (δ, with error $\pm$ 0.001 ppm) shows a sigmoidal (having an average of 40 chemical shifts in each titration region) behavior (Figure S1 in the Supporting Information). The pK_a determination (Table 1) is based on the Hill plot analysis[4,30] using the equation pH = log(($1 - \alpha$)/α) + pK_a, where α represents a fraction of the protonated or deprotonated species. The value of α is calculated from the change of chemical shift relative to the neutral (N) or deprotonated (D) state at a given pH ($\Delta_P = \delta_N - \delta_{obs}$ for protonation and $\Delta_D = \delta_D - \delta_{obs}$ for deprotonation, where δ_{obs} is the experimental chemical shift at a particular pH), divided by the total change in chemical shift between neutral and protonated (P) or deprotonated (D) state (Δ_T). So the Henderson−Hasselbalch type equation[4,24,30] can then be written as pH = log(($\Delta_T - \Delta_{P/D}$)/$\Delta_{P/D}$) + pK_a. The pK_a is calculated from the linear regression analysis of the Hill plot (Figure S2 in the Supporting Information). Moreover, we have also shown the pH-dependent fraction protonation[42] [$f_P = \Delta_P/\Delta_T$] as well as fraction deprotonation [$f_D = \Delta_D/\Delta_T$]. The equation used for the nonlinear regressional analyses is $f_{P/D} = 1/1 + 10^{(pH-pKa)}$ (Figure S3 in the Supporting Information).

(C) Free Energy of Protonation/Deprotonation. The equation $\Delta G^{\circ}_{pK_a} = 2.303RT{*}pK_a$[24,25] shows the estimation of free energy of protonation/deprotonation at pH = pK_a for compounds **1**−**10** (Table 1). So the ΔpK_a gives the estimation of $\Delta\Delta G^{\circ}_{pK_a}$ due to protonation/deprotonation.

(D) pH-Dependent Sugar Conformation Using PSEUROT (v5.4). The conformational analyses of the furanose moiety of **1**−**10** in acidic (pH = 1.9), neutral (pH = 6.6), and alkaline (pH = 10.4) state have been performed by the computer program PSEUROT (v5.4)[6] using experimental $^3J_{HH}$. It is based on the generalized Karplus equationas[6] and pseudorotational[6] (using the pseudorotation equations for the five membered ring: $\nu_j = \Psi_m \cos(P + 4\pi(j-2)/5)$ [$0 \leq j \leq 4$] and tan $P = (\nu_4 + \nu_1 - \nu_3 - \nu_0)/3.077\nu_2$, where ν_j is the endocyclic torsion). It calculates the best fit of the five conformational parameters [P, Ψ_m for both N- and S-type pseudorotamers and the mole fractions of N (x_N) or S (x_S) conformers] to the three experimental $^3J_{H,H}$ [viz. $^3J_{1'2'}$, $^3J_{2'3'}$, and $^3J_{3'4'}$]. The calculated mole fractions of N (x_N) or S (x_S) conformers were used to calculate the free energy of N $\leftrightarrows$ S pseudorotational equilibrium ($\Delta G^{\circ}_{N/S(298K)}$, in kJ mol^{-1}) using Gibb's equation: $\Delta G^{\circ}_{N/S(298K)} = -RT \ln K$, where $K = (x_N/x_S)$. See Table S3 in the Supporting Information for details of the PSEUROT (v5.4) estimated parameters for **1**−**10**.

(E) pH-Dependent Free Energy of Stacking. Free energy of stacking ($\Delta\Delta G^{\circ} \cong \Delta G^{\circ}_{stacking}$, in kJ mol^{-1}) for **1**−**6** at neutral (pH = 6.6), acidic (pH = 1.9), and alkaline (pH = 10.4) state have been calculated using relation: $\Delta\Delta G^{\circ} \cong \Delta G^{\circ}_{stacking} = [\Delta G^{\circ}_{N/S(298K)}]_{NpN'} - [\Delta G^{\circ}_{N/S(298K)}]_{NpEt}$, where NpN′ and NpEt signify 3′-nucleotidyl moiety (in bold) of 3′-5′ dinucleoside monophosphate (**Gp**A, **Ap**G, **Ap**U, **Up**A, **Up**C, and **Cp**U; see Chart 1) and nucleoside 3′-ethyl phosphate (**N**pEt with N = A, G, U, and C; see Chart 1), respectively. See part E of the Experimental Section and Tables S1 and S2 in the Supporting Information for details of calculation of $\Delta G^{\circ}_{N/S(298K)}$.

(F) Calculations of the Dimerization Shift. The dimerization shift[17−19] ($\delta_{NpEt} - \delta_{NpN'}$, in ppm) have been calculated by subtracting chemical shift of the aromatic protons of nucleoside 3′-ethyl phosphate

(29) For review: Patel, D. J.; Suri, A. K. *Rev. Mol. Biotechnol.* **2000**, *74*, 39.
(30) Legault, P.; Pardi, A. *J. Am. Chem. Soc.* **1997**, *119*, 6621 and references therein.
(31) Ravindranathan, S.; Butcher, S. E.; Feigon, J. *Biochemistry* **2000**, *39*, 16026.
(32) Drohat, A. C.; Stivers, J. T. *Biochemistry* **2000**, *39*, 11865.
(33) Nakano, S.; Chadalavada, D. M.; Bevilacqua, P. C. *Science* **2000**, *287*, 1493, and references therein.
(34) Xiong, L.; Polacek, N.; Sander, P.; Böttger, E. C.; Mankin, A. *RNA* **2001**, *7*, 1365.
(35) Ryder, S. P.; Oyelere, A. K.; Padilla, J. L.; Klostermeier, D.; Millar, D. P.; Strobel, S. A. *RNA* **2001**, *7*, 1454, and references therein.
(36) Narlikar, G. J.; Herschlag, D. *Annu. Rev. Biochem.* **1997**, *66*, 19, and references therein.
(37) For review: Ramakrishnan, V. *Cell* **2002**, *69*, 557.
(38) Leninger, A. L.; Nelson, D. L.; Cox, M. M. *Principles of Biochemistry*, 2nd ed.; Worth Publishers Inc.: New York, 1993.
(39) For review: Grinstaff, M. W. *Angew. Chem., Int. Ed.* **1999**, *38*, 3629.
(40) For review: Giese, B. *Acc. Chem. Res.* **2000**, *33*, 631.
(41) Guerra, C. F.; Bickelhaupt, F. M. *Angew. Chem., Int. Ed.* **1999**, *38*, 2942.

(42) Felemez, M.; Bernard, P.; Schlewer, G.; Spiess, B. *J. Am. Chem. Soc.* **2000**, *122*, 3156.
(43) It has been observed in the inter- and intramolecular stacking interaction between indole and adeninium ring that when adenine base by protonation or methylation (at N^1) takes up adeninium form, the LUMO energy of adenine [+0.1367 au] is significantly lowered by quarternization of protonated nitrogen [−0.1182 au]. Such protonation saves energy of +0.2549 au (ca. 159.95 kcal mol^{-1}) in interaction with HOMO [−0.3996 au] of the indole ring. It has been found that in these stacked pairs, the indole ring more strongly interacts with the pyrimidine rather than imidazole part of the adeninium ring. Ishida, T.; Shibata, M.; Fuji, K.; Inoue, M. *Biochemistry* **1983**, *22*, 3571.
(44) Xu, D.; Norlund, T. M. *Biophys. J.* **2000**, *78*, 1042.

(δ_{NpEt}), **7**−**10**, from that of 3′-nucleotidyl unit of 3′−5′ dinucleoside monophosphate ($\delta_{NpN\_}$), **1**−**6**, at neutral (pH = 6.6), acidic (pH = 1.9), and alkaline (pH = 10.4) state (see Figure S5 in the Supporting Information).

Supporting Information Available: Figures S1−S6 showing, for compounds **1**−**10**, plots of aromatic proton chemical shift as a function of pH, the Hill plot analysis of the pH-dependent shifts of aromatic protons to calculate the pK_a of nucleobase, and plots of fraction protonation or deprotonation as a function of pH and, for dimers **1**−**6**, a plot of the chemical shift change over the pH-range, $\Delta\delta$, in comparison with monomers **7**−**10**, showing a direct evidence for atom−$\pi\sigma$ interaction between the nearest neighbor necleobases and bar plots showing dimerization shift of the aromatic protons and Tables S1−S3 listing, for compounds **1**−**10**, pH-dependent endocyclic $^3J_{HH}$, the percentage population of N-type pseudorotamer (% N), the corresponding free energy ($\Delta G^\circ_{N/S(298K)}$) and $\Delta G^\circ_{stacking}$, and pseudorotational parameters determined by PSEUROT (v5.4) calculations at different pH, and the dimerization shift estimated from ^1H chemical shift at 298 K for aromatic protons of monomers **7**−**10**, in comparison with dimers **1**−**6**, at different pH. This material is available free of charge via the Internet at http://pubs.acs.org.

JA026831H